DOI: 10.1002/ejic.201000516

Structural Characterization of Novel *ortho*-Lithiated Imines

John F. Beck,[a] Abdollah Neshat,[a] and Joseph A. R. Schmidt*[a]

Keywords: Lithiation / Ligand design / Schiff bases / Imines / Coordination polymer

ortho-Metallated imines are commonly used as ligands for late transition metals. Unfortunately, not all metals, such as titanium, zirconium, and niobium, can undergo the necessary oxidative addition reactions to form the desired *ortho*-metallated complexes directly. Therefore, a synthetic methodology allowing easy access to this binding mode from simple early transition metal halides via an *ortho*-lithiated imine precursor is desirable. *ortho*-Lithiation of benzylamines and other systems has been well studied; in contrast, that of imines is poorly developed. However, inclusion of a 3,4-methylenedioxy group on phenyl imines allows for straightforward lithiation and simple isolation of the *ortho*-lithiated imines. NMR spectroscopy and single-crystal X-ray diffraction allowed for the structural elucidation of the clustering in these lithium complexes. It has been determined that the nature of the imine nitrogen substituent has a profound effect on the clustering of the lithiated imines. Alkyl (Cy, *t*Bu) substituents clustered in a tetrameric form, whereas aryl (2,6-$R_2C_6H_3$; R = Me, Et, *i*Pr) substituents formed dimers that exhibited long-range ordering in the solid state as coordination polymers. The introduction of coordinating solvent, such as dimethoxyethane and diethyl ether, changed the long-range order of the coordination polymer and in some cases, forced the formation of discrete dimeric lithium complexes. Lithium NMR spectroscopy indicates that in solution the coordination polymer breaks up to form discrete dimers. These complexes also display a pronounced decrease in the ring bond angle of the aromatic carbon atom directly attached to the lithium atom, which indicates an increase in the p-character of the carbon–lithium bond.

Introduction

The first examples of the *ortho*-lithiation of heterosubstituted arenes were noted by Gilman[1,2] and Wittig[3] in the late 1930s. Many functional groups have since been identified as good *ortho*-directing moieties, and the general magnitude of their effect on *ortho*-lithiation has been determined as $CONEt_2 > CH_2NMe_2 > OCH_3 > F$.[4–7] Absent from this list is the imine functionality due to its generally poor *ortho*-directing ability and the usual formation of undesirable side products upon its use.[8,9] There are some examples of *ortho*-lithiated imines as synthetic intermediates in organic synthesis,[10–13] but isolation and structural characterization of these compounds remains notably absent from the literature. A search of the Cambridge Structural Database shows no examples of structurally characterized *ortho*-lithiated imines, but does yield a few examples of the closely related *ortho*-lithiated phenyloxazolines.[14–17] These include species with either one or two oxazoline groups located *ortho* to the lithiated phenyl carbon atom.

In 1975, Ziegler and Fowler successfully *ortho*-lithiated piperonal cyclohexylimine using *n*-butyllithium (*n*BuLi) and isolated the subsequent product of its reaction with iodine.[18] This compound and others prepared by more traditional lithium/halide exchange reactions have been used in the total synthesis of (±)-steganacin, an antileukemic natural product.[19] Flippin and co-workers have *ortho*-lithiated a wider range of imines employing lithium 2,2,6,6-tetramethylpiperidide and isolated the products of their subsequent reactions with numerous electrophiles in high yields.[11] Many of the known *ortho*-lithiated imines incorporate more conventional *ortho*-directing groups, such as the methoxy group. Given its electronic similarities to the methoxy group, the methylenedioxy functionality pioneered by Ziegler and Fowler undoubtedly has an *ortho*-directing effect. Indeed, several *ortho*-lithiated compounds have been isolated incorporating the methylenedioxy group, including amides,[20] amines,[21] and thioethers.[22] Thus, it seemed likely that the methylenedioxy group could be used as an *ortho*-directing moiety to assist in the synthesis and isolation of these elusive *ortho*-lithiated imines.

In our recent work, we have shown that 3,4-methylenedioxyphenyl imines can be readily synthesized by Schiff base condensation reactions of the related aldehydes and ketones. *ortho*-Lithiation of these imines proceeds readily to yield the deprotonated species, where regiospecific lithiation occurs at the position mutually *ortho* to both the methylenedioxy and imine groups.[23,24] To date, we have investigated the use of these anionic units as ancillary ligands in compounds of titanium, zirconium, niobium, and tantalum.[23–25] Due to the interesting NMR spectroscopic features observed for these *ortho*-lithiated imines and the general lack of structurally characterized examples of this

[a] Department of Chemistry, The University of Toledo
2801 W. Bancroft St. MS 602, Toledo, Ohio 43606-3390, USA
E-mail: Joseph.Schmidt@utoledo.edu

Supporting information for this article is available on the WWW under http://dx.doi.org/10.1002/ejic.201000516.

class of molecules, we embarked on a study of the molecular structure of these *ortho*-lithiated imines, crystallized from a wide variety of nonpolar solvents. In this contribution, we show the results of the crystallization of these species from both coordinating and noncoordinating solvents, the impact of steric bulk of the imine substituent, and the overall clustering observed in a series of eight *ortho*-lithiated imines.

Results and Discussion

A series of eight imines was prepared by using the Schiff base condensation reactions of either 3′,4′-methylenedioxyacetophenone or piperonal with various primary amines in refluxing toluene along with a catalytic amount of *para*-toluenesulfonic acid. The only exception was **H-L^2**, which, because of the low boiling point of *tert*-butylamine, was synthesized from an imido/oxo exchange reaction between Ti(N*t*Bu)Cl_2py_3 and 3′,4′-methylenedioxyacetophenone.[23] The subsequent lithiation of **H-L$^{1–8}$** was performed in pentane at reduced temperature (Scheme 1), although for the imines with sterically very bulky groups bound to the nitrogen atom, such as 2,6-*i*$Pr_2C_6H_3$, lithiation was effective at room temperature with no reduction in yield or purity. Of this series of eight *ortho*-lithiated imines, **Li-L^3** was found to be comparatively unstable, decomposing into unidentifiable products even at low temperature. The simple inclusion of a methyl group on the imine carbon atom to produce the related ketimine (**Li-L^4**) dramatically increased its stability in organic solvents. This seems to indicate a significant steric contribution to the overall stability of these lithium complexes in solution. In contrast, no *ortho*-lithiated ketimines could be isolated from attempts to lithiate the related imines bearing phenyl or 4-MeC_6H_4 substituents on the imine nitrogen atom. Each of the successfully lithiated imines exhibited low solubility in pentane, precipitating from the reaction mixture as a powder soon after the addition of *n*BuLi in good yields with a high degree of purity. Lithiation can also be successfully carried out in toluene and ethereal solvents. THF cannot be used as a solvent at room temperature because of the acidic nature of its α-proton that leads to protonation of the lithiated imine, although it did perform well at –78 °C.

In an effort to more deeply understand the clustering of these *ortho*-lithiated imines, we undertook a project to crystallographically characterize the different structural motifs displayed by these complexes. Specifically, we wanted to understand the effects caused by changes in ligand substituents (group bound to the nitrogen atom of imine, aldimine vs. ketimine) and the impact of crystallization from coordinating and noncoordinating solvents. The structure of **Li-L^1** was determined to be a tetramer in the solid state when recrystallized from toluene/pentane. Its four lithium atoms were found to be in a pseudotetrahedral arrangement, where each lithium atom in the tetramer is four-coordinate, bound to a nitrogen atom of one ligand, two bridging aryl carbon atoms from two different ligands and the oxygen atom of a fourth ligand (Figure 1). **Li-L^2** was crystallized from diethyl ether, and its X-ray structure was found to be nearly identical to that of **(Li-L^1)$_4$**. These two analogous structures show that one methylene proton of the methylenedioxy ring is oriented towards the imine alkyl group, whereas the other points toward the aryl backbone. Because of this dissymmetry, in the ^{1}H NMR spectrum of **(Li-L^1)$_4$**, the two methylene protons of the five-membered ring are observed as singlets at δ = 5.47 and 4.74 ppm. Heteronuclear multiple quantum coherence NMR spectroscopy confirmed that both singlets couple to the same carbon atom. The pronounced upfield chemical shift of one of these singlets can be attributed to ring current effects due to the close proximity of the proton to the centroid of the adjacent aryl backbone (ca. 3.96 Å in the solid state).[26–28] This is in remarkable contrast to the ^{1}H NMR spectra observed for the lithiated aryl imines (**Li-L$^{3–8}$**). For the lithiated aryl imines, in all cases the two protons of the methylenedioxy unit were found to be equivalent on the solution NMR timescale. Also, spectra of these *ortho*-lithiated aryl imines all showed reasonably upfield-shifted methylenedioxy proton signals. For the initial imine, these proton signals appeared at $\delta \approx$ 5.2 ppm, whereas they shifted to $\delta \approx$ 4.9 ppm in the lithium complexes. These methylene protons were observed to be

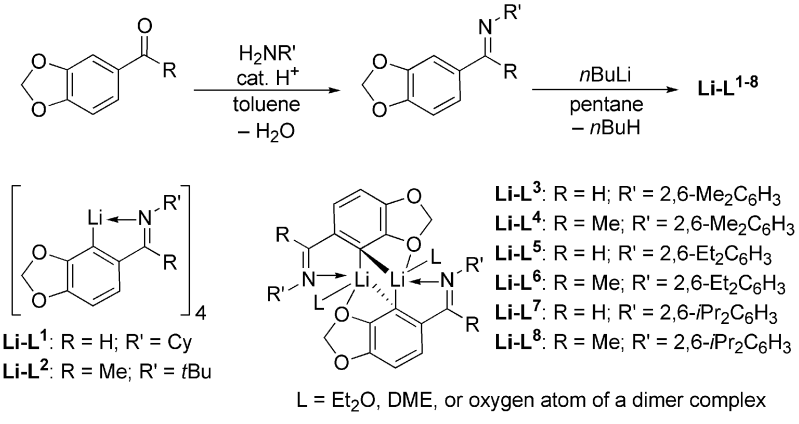

Scheme 1. Synthesis of lithiated imines from corresponding ketones or aldehydes.

chemically equivalent, although their signals do appear slightly broadened in the ^{1}H NMR spectra. We attribute this broadening to the motion of the flexible methylenedioxy ring, and this broadness is not observed for other proton signals in the lithium complexes. The effect of this motion is to average the chemical environment of these two protons about the mirror plane of the ligand. This averaging is not possible for the tetrameric **(Li-L^1)$_4$** and **(Li-L^2)$_4$** structures as the two faces of the planar ligand are not equivalent in these structures. Thus, based on the differences in NMR spectra, a different clustering motif must be present in solution for the *ortho*-lithiated aryl imines.

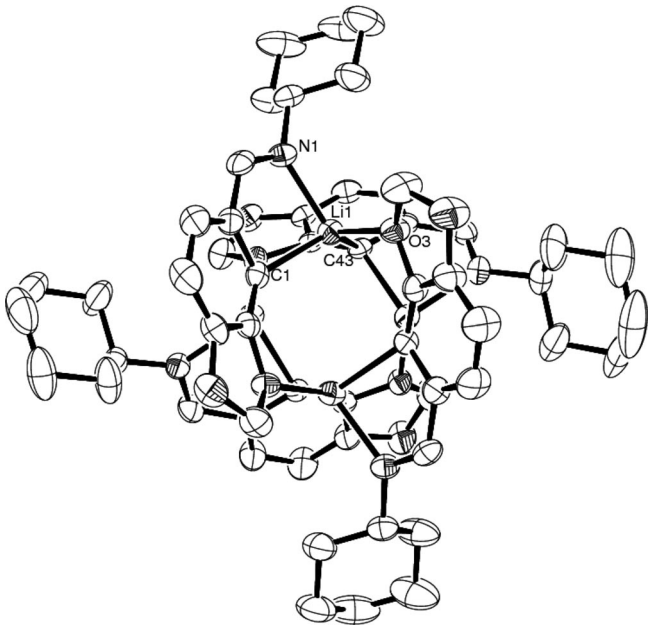

Figure 1. ORTEP diagram of **(Li-L^1)$_4$** with thermal ellipsoids drawn at 50% probability. Hydrogen atoms and toluene solvent molecule have been omitted for clarity. Li1 displays pseudotetrahedral geometry, bonding to C1, O3, N1, and C43.

As the *ortho*-lithiated aryl imines all displayed similar ^{1}H NMR spectra in C_6D_6, we crystallized a representative collection of these species from various coordinating and noncoordinating solvents. Three *ortho*-lithiated aryl imine complexes (**Li-L^6**, **Li-L^7**, and **Li-L^8**) were crystallized from noncoordinating solvents. These three compounds displayed similar solid-state structures, forming long polymeric chains of dimeric units. In each dimer within the chain, two lithium centers are bound to the bridging *ortho*-carbon atoms of two ligands, as well as a nitrogen atom from one ligand and an oxygen atom from the methylenedioxy ring of the other ligand. The methylenedioxy oxygen atom not involved in bonding within the dimer forms a dative bond to a lithium center on an adjacent dimer to link the chain. Thus, two different types of dimers exist within the polymeric chain: "donor" dimers that provide electron density from the oxygen donor atom and "acceptor" dimers with lithium atoms coordinated by this oxygen donation. Overall, an alternating linkage of "donor" and "acceptor" dimers forms the polymeric chains (Figure 2). The two types of dimers give rise to two chemically inequivalent lithium centers in the solid state. The lithium centers of the "donor" dimer are square-planar and the lithium centers of the "acceptor" dimer are square-pyramidal (Figure 3). However, ^{7}Li{^{1}H} NMR spectroscopy in C_6D_6 shows only one resonance in solution at room temperature (Table 1). Variable-temperature NMR experiments (C_7D_8) showed no changes between 80 °C and –30 °C, although significant precipitation was observed in the NMR tube upon cooling. We believe the observation of a single lithium signal is due to the dissolution of the polymeric chains to form discrete dimers, rather than higher-order clusters, in solution. The high degree of solubility of these *ortho*-lithiated imines in toluene, benzene, and ethers also supports the likelihood of a smaller cluster in solution. Within each dimer, there is a time-averaged mirror plane of symmetry and an inversion center relating each of the four methylene protons and accounting for the single resonance observed for these methylene protons in the spectra of the *ortho*-lithiated imines. Once again, this upfield chemical shift can be attributed to a π interaction between the methylene protons and the aromatic system of the second ligand in the dimer.[27] For example, the methylenedioxy protons are located an average of approximately 3.3 Å from the centroid of the aryl ring of the imine in **(Li-L^6)$_2$**. Thus, as in **(Li-L$^{1-2}$)$_4$** the ring current of the aromatic group is shielding the methylene protons and shifting their signals upfield in the observed NMR spectra.

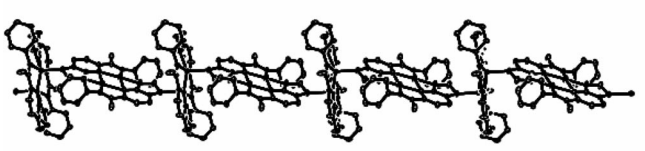

Figure 2. ORTEP diagram of coordination polymer of **(Li-L^8)$_2$** with thermal ellipsoids drawn at 50% probability; hydrogen atoms, isopropyl groups and benzene solvent molecule have been omitted for clarity.

Unlike the alkyl imine **Li-L^2**, crystallization of the aryl imines from coordinating solvents resulted in materials in which ethereal solvent molecules were retained in the cluster by dative bonding to the lithium centers. In no case was the dimeric core structure disrupted, but disruption of the polymeric chains or additional coordination to the lithium centers was observed. For example, when **Li-L^4** was crystallized from diethyl ether, a nonpolymeric, but dimeric structure was observed in the solid state: **(Li-L^4·Et$_2$O)$_2$**. The crystallographically equivalent lithium centers display distorted square-pyramidal geometry (τ = 0.105, vide infra) with each lithium atom bearing one diethyl ether ligand arranged on opposing faces of a dimer similar to those discussed above (Figure 4). Interestingly, when larger 2,6-disubstituted aryl groups were incorporated as the imine substituent [2,6-Et$_2$C$_6$H$_3$ (**Li-L^6**) instead of 2,6-Me$_2$C$_6$H$_3$ (**Li-L^4**)], the polymeric nature of the complex in the solid state

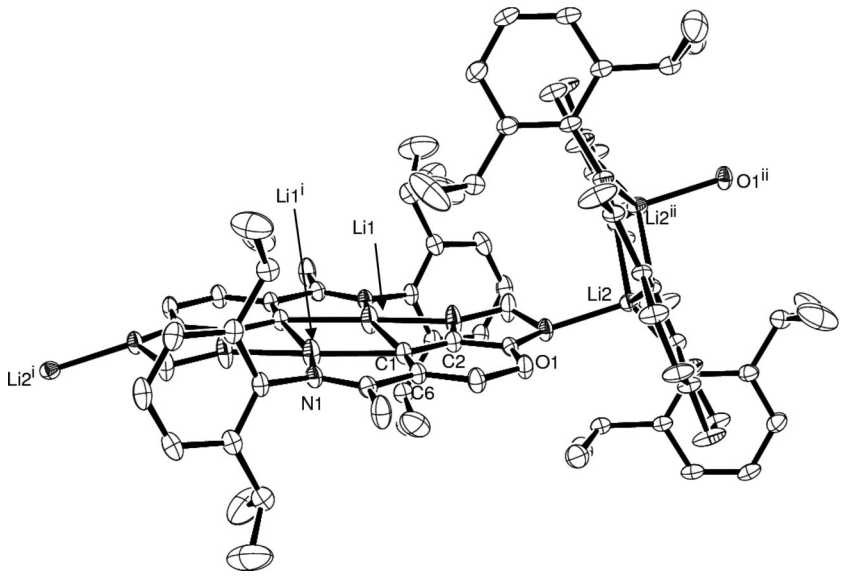

Figure 3. ORTEP diagram of **(Li-L^8)$_2$** with thermal ellipsoids drawn at 50% probability; hydrogen atoms and benzene solvent molecule have been omitted for clarity. Note the presence of the square-planar lithium atom Li1 in the "donor" dimer and the square-pyramidal lithium atom Li2 in the "acceptor" dimer. Atoms labeled with "i" and "ii" are generated by the following symmetry operators: $-x + 1$, $-y$, $-z$; $-x + 1$, $-y$, $-z + 1$.

Table 1. Lithium NMR chemical shifts (C_6D_6).

Compound	^{7}Li{^{1}H} [ppm]
(Li-L^1)$_4$	2.91
(Li-L^2)$_4$	2.82
(Li-L^4)$_2$	3.67
(Li-L^5)$_2$	2.68
(Li-L^6)$_2$	4.08
(Li-L^7)$_2$	3.90
(Li-L^8)$_2$	4.12
(Li-L^8)$_2$·DME	3.84

is preserved to give **(Li-L^6)$_2$·Et$_2$O**. In fact, within this polymeric chain, there is little or no change to the "acceptor"dimer units, being nearly isostructural to the "acceptor" dimer in **(Li-L^6)$_2$**. However, the lithium centers of the "donor" dimers are now found to be five-coordinate square-pyramidal (τ = 0.282, vide infra) with diethyl ether ligands coordinated on opposing faces in a very similar manner to **(Li-L^4·Et$_2$O)$_2$**.

When dimethoxyethane (DME) was used as a component of the reaction solvent for the imine *ortho*-lithiation, NMR spectroscopy showed that 1 equiv. of DME remains for every two lithiated ligands. This was subsequently confirmed by elemental analysis. The structure in the solid state shows a dimeric complex (Figure 5), which in this case is very similar to that observed when **Li-L^4** was crystallized from diethyl ether. Each lithium center has a square-pyramidal geometry (τ = 0.018, vide infra) with one DME oxygen atom coordinated on each opposing face of the dimer. Two separate DME molecules coordinate to this core dimeric structure. The second oxygen atom from each of these DME ligands then coordinates to another dimer unit to

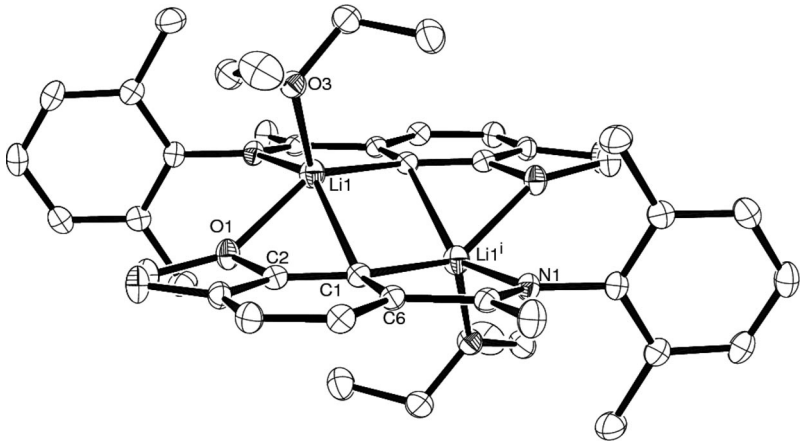

Figure 4. ORTEP diagram of **(Li-L^4·Et$_2$O)$_2$** with thermal ellipsoids drawn at 50% probability, crystallized from diethyl ether. Hydrogen atoms have been omitted for clarity. Atoms labeled with "i" are generated by the following symmetry operator: $-x + 2$, $-y$, $-z + 1$.

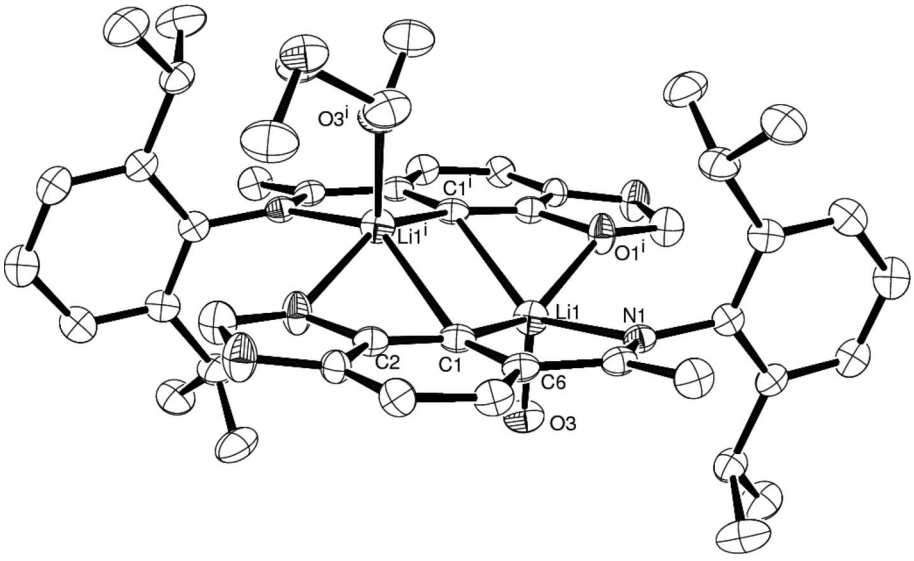

Figure 5. ORTEP diagram of **(Li-L^8)$_2$·DME** with thermal ellipsoids drawn at 50% probability; hydrogen atoms have been omitted for clarity. Atoms labeled with "i" are generated by the following symmetry operator: $-x + 1, -y + 1, -z + 1$.

create a coordination polymer made up of alternating lithium dimers and bridging DME ligands. This bridging binding mode was previously observed by Jones and Nixon[29] and is related to the chelating and bridging modes commonly observed with tetramethylethylenediamine ligands.[30,31] Furthermore, the complex **(Li-L^8)$_2$·DME** retains DME after exposure to vacuum, unlike **(Li-L^4·Et$_2$O)$_2$**, which loses diethyl ether readily under vacuum.

For five-coordinate complexes, τ is often used as a measure to quantify the degree to which the coordination geometry relates to that of an idealized square-pyramidal ($\tau = 0$) or trigonal-bipyramidal ($\tau = 1$) arrangement.[32] For the five-coordinate lithium centers reported herein, τ is close to zero in all cases (Table 2), indicating a minimal distortion around the metal center from that of the idealized square-pyramidal geometry. The degree of intermolecular vs. intramolecular lithium solvation can be expressed by a parameter known as the twist angle.[33] The twist angle is given as the angle between the planes defined by the two lithium centers and the bridging donor carbon atom and the plane of the aryl ring of the ligand. If these two planes are coplanar the twist angle is 0° (indicating strong intramolecular solvation), whereas a perpendicular arrangement gives a twist angle of 90° (intermolecular solvation).[17,33–36] The twist angles for the "donor" dimers range from 0.8–5.9° as expected for square-planar metal complexes, whereas the twist angles for the "acceptor" dimers are larger (16.0–29.6°), indicating a much higher degree of intermolecular solvation from the "donor" dimers to the lithium ions (Table 3). Additionally, the five-coordinate complexes incorporating ethereal ligands, rather than "donor" dimers, have slightly larger twist angles, although this difference is most likely a reflection of the significant difference in steric bulk between the donor dimer and diethyl ether or DME, rather than a difference in oxygen donor character. Sterics also play an important role in maintaining the planarity of the "donor" dimer. As steric bulk increases, a decrease in the twist angle of the "donor" dimers occurs, probably due to minimization of the steric interactions between the bulky groups at the 2- and 6-positions of the aromatic rings. For example, the ketimine "donor" dimer (**Li-L^8**) has the most planar character with a twist angle of only 0.8°; however, the structurally analogous aldimine (**Li-L^7**) has a twist angle of 5.2°. Thus, inclusion of the methyl group on the imine carbon atom seems to impact the solvation of the lithium center.

Table 2. τ values for five-coordinate lithium centers.

Compound	τ
(Li-L^4·Et$_2$O)$_2$	0.105
(Li-L^6)$_2$	0.105
(Li-L^6)$_2$·Et$_2$O	0.087, 0.282[a]
(Li-L^7)$_2$	0.245
(Li-L^8)$_2$	0.131
(Li-L^8)$_2$·DME	0.018

[a] Donor dimer with diethyl ether bond.

Table 3. Twist angles for lithium complexes.

Compound	Twist angle [°]
(Li-L^4·Et$_2$O)$_2$	30.8(1)
(Li-L^6)$_2$	5.9(1), 29.6(1)[a]
(Li-L^6)$_2$·Et$_2$O	35.0(2), 27.2(2)[a]
(Li-L^7)$_2$	5.2(1), 21.5(1)[a]
(Li-L^8)$_2$	0.8(2), 16.0(2)[a]
(Li-L^8)$_2$·DME	28.6(2)

[a] Acceptor dimer.

An examination of the metrical parameters from the crystal structures shows that the carbon–lithium bond lengths are similar for all the lithium complexes (Table 4). This bridging binding motif is observed in many lithium complexes.[14,37,38] There is a slight elongation of the carbon–lithium bond *trans* to the nitrogen donor in both the

square-planar and square-pyramidal structures in comparison to the carbon–lithium bond *trans* to the oxygen donor. This is due to the stronger *trans* effect of nitrogen compared to that of oxygen. The additional elongation observed in the carbon–lithium bond *trans* to nitrogen atom for the square-pyramidal lithium centers is also due to movement of the lithium atom out of the basal plane, in order to form the square-pyramidal geometry. This distortion causes a lengthening of the carbon–lithium bonds compared to those with square-planar geometry. This is especially pronounced in **(Li-L^4·Et$_2$O)$_2$**, where the carbon–lithium bonds range from 2.153(2) Å *trans* to O to 2.640(2) Å *trans* to N. Note that this complex also shows the largest twist angle of 30.8(1)°.

Table 4. Selected bond lengths [Å] and angles [°].[a]

Compound	Li1–C[b]	Li1–C[c]	Li1–N1	C2–C1–C6	C1–Li1–N1
(Li-L^1)$_4$	2.215(6)	–	2.051(6)	109.7(3)	85.0(2)
(Li-L^2)$_4$	2.202(6)	–	2.061(6)	110.2(3)	85.0(2)
(Li-L^4·Et$_2$O)$_2$	2.153(2)	2.640(2)	2.108(2)	109.9(1)	80.99(8)
(Li-L^6)$_2$	2.247(5)	2.447(5)	2.059(5)	109.5(2)	83.8(2)
(Li-L^6)$_2$·Et$_2$O	2.259(4)	2.323(4)	2.079(4)	109.7(2)	79.6(1)
(Li-L^7)$_2$	2.132(5)	2.464(6)	2.038(5)	109.2(2)	85.7(2)
(Li-L^8)$_2$	2.146(3)	2.475(3)	2.025(3)	109.6(1)	83.6(1)
(Li-L^8)$_2$·DME	2.178(4)	2.538(4)	2.137(4)	110.1(2)	80.4(1)

[a] For **Li-L$^{6–8}$**, values shown are for the "donor" dimers. [b] Lithium–carbon bond *trans* to O for aryl imines. [c] Lithium–carbon bond *trans* to N for aryl imines.

For comparison, we include the crystal structure of **H-L^8**, noting that the ligand itself undergoes various substantial changes upon deprotonation. The protic ligand (**H-L^8**) has a C2–C1–C6 bond angle of 117.4(1)°. This is a slight deviation from the expected value of 120°. It is coupled to an elongation of the C1–C6 bond in the aromatic system and is caused by resonance effects between the conjugated imine and the aromatic system. Upon deprotonation, C1 undergoes significant changes, and the C2–C1–C6 bond angle decreases from 117.4(1)° (**H-L^8**) to 109.5(1)° (**Li-L^8**). This decrease in bond angle indicates an increase in the p-character of the carbon bond to the metal atom.[33,36,39–43] Concurrently, the planarity of the aromatic ring is maintained by corresponding increases in other carbon–carbon bond lengths and angles. This decrease of the C2–C1–C6 bond angle upon lithiation is commonly observed, although an angle of 109° is among the smallest reported. Additional stabilizing effects are likely provided by contributions from the lone pair on the oxygen atom and resonance with the imine, leading to the excellent stability observed in the complexes reported herein.

Conclusions

Several *ortho*-lithiated alkyl and aryl imines were synthesized and structurally characterized. To the best of our knowledge, these are the first examples of isolated and structurally characterized *ortho*-lithiated imines, although some *ortho*-lithiated phenyloxazolines have been previously reported.[17] In general, clustering in the solid state was dependent upon both the crystallization solvent used and the substituent on the imine nitrogen atom. Recrystallization from noncoordinating solvents led to the formation of coordination polymers for the *ortho*-lithiated aryl imines, where individual dimeric units were linked coordinatively to form infinite chains, giving rise to two types of lithium centers – square-planar and square-pyramidal. Crystallization from ethereal solvents, such as diethyl ether, led to the formation of discrete dimeric lithium complexes with square-pyramidal lithium centers when the nitrogen substituent was 2,6-Me$_2$C$_6$H$_3$. When sterically more bulky nitrogen substituents were used, such as 2,6-Et$_2$C$_6$H$_3$, the dimers formed polymeric chains even in the presence of diethyl ether. In the case of **(Li-L^6)$_2$·Et$_2$O** the same dimers are observed as in the polymer derived from crystallization from noncoordinating solvents, but the remaining open coordination sites of the square-planar lithium atoms were filled by diethyl ether ligands. The *tert*-butyl and cyclohexyl derivatives both formed tetramers in the solid state; **(Li-L^1)$_4$** and **(Li-L^2)$_4$** were crystallized from toluene/pentane and diethyl ether, respectively. Lithium NMR spectra showed only one resonance in the solution state for each complex, indicating disruption of the polymeric chains in solution. All aryl imine complexes likely exist as dimers in solution and the alkyl imines as tetramers. Overall, we have shown that *ortho*-lithiated imines can be readily synthesized and isolated, and their rich structural chemistry, dependent on crystallization solvent and ligand substituent, corresponded well to the steric and electronic features of the various isolated complexes.

Experimental Section

General Methods and Instrumentation: All manipulations involving lithium reagents were performed under N_2 by using standard glovebox and Schlenk techniques. Solvents were dried before use; pentane and toluene were passed through columns of molecular sieves (4 Å) and sparged with nitrogen. Diethyl ether was passed through columns of activated alumina and molecular sieves (4 Å) and sparged with nitrogen. DME and [D$_6$]benzene were dried with sodium metal, freeze-pump-thawed three times, and vacuum-distilled. *tert*-Butylamine was dried with calcium hydride, freeze-pump-thawed three times, and distilled under reduced pressure. Piperonal, 3′,4′-methylenedioxyacetophenone, and *p*-toluenesulfonic acid were purchased from Acros and used as received. ^{1}H and ^{13}C{^{1}H} NMR spectroscopic data were obtained with a 600 MHz Inova NMR spectrometer at ambient temperature at 599.9 MHz for ^{1}H NMR and 150.8 MHz for ^{13}C{^{1}H} NMR spectroscopy. All NMR spectra were recorded by using C_6D_6 as the solvent. ^{1}H NMR shifts are given relative to C_6D_5H (δ = 7.16 ppm), and ^{13}C NMR shifts are given relative to C_6D_6 (δ = 128.1 ppm). Unless otherwise noted, all coupling constants are $^3J_{HH}$. ^{7}Li NMR spectra are given relative to an external LiCl (3.00 M in D_2O) standard (δ = 0.00 ppm) and were obtained with a 400 MHz VXRS NMR spectrometer at 155.4 MHz. IR samples were prepared as Nujol mulls and

measured between KBr plates with a Perkin–Elmer XTL FTIR spectrophotometer. Melting points were observed with a capillary melting-point apparatus (Uni-Melt) in sealed capillary tubes and are uncorrected. X-ray structure determinations were performed at the Ohio Crystallographic Consortium housed at The University of Toledo. Elemental analyses were determined by Desert Analytics, Tucson, AZ, or Galbraith Laboratories, Inc., Knoxville, TN.

CCDC-776002, -776003, -776004, -776005, -776006, -776007, -776008, -776009, -776010 contain the supplementary crystallographic data for this paper. These data can be obtained free of charge from The Cambridge Crystallographic Data Centre via www.ccdc.cam.ac.uk/data_request/cif.

General Procedures for Ligand Synthesis and Lithiation

Ligand Synthesis: The appropriate amount of a primary amine (1–2 equiv.) was added to a solution of either 3′,4′-methylenedioxyacetophenone or piperonal (1 equiv.) in toluene. A catalytic amount of *p*-toluenesulfonic acid was added, and the reaction mixture was heated to reflux for 2 d (piperonal) or 3 d (3′,4′-methylenedioxyacetophenone). A Dean–Stark trap was used to collect water generated in the course of the reaction, and the progress of the reaction was monitored by the volume of water collected. The reaction mixture was allowed to cool and neutralized with a saturated aqueous $NaHCO_3$ solution and washed twice with deionized water. The solvent was then removed under reduced pressure and the residue distilled to yield the final product. The only exception (**H-L^2**) was prepared by imido/oxo exchange of Ti(N*t*Bu)Cl_2py_3 and 3′,4′-methylenedioxyacetophenone due to the volatility of *tert*-butylamine. Compounds **H-L$^{1–2}$**, **H-L^4**, and **H-L$^{6–8}$** were prepared according to previously published methods.[18,23,24]

Ligand Lithiation: The imine (1 equiv.) was dissolved in pentane, cooled to –78 °C, and *n*BuLi (0.99 equiv.) slowly added. As the reaction proceeded, the lithiated product precipitated as a powder, which was subsequently washed with pentane to yield the final lithiated imine. The use of pentane/DME (3:1) as a reaction solvent under identical conditions yielded the DME adduct **(Li-L^8)$_2$·DME**, which also precipitated from the reaction solvent. Compounds **Li-L$^{1–2}$**, **Li-L^4**, and **Li-L$^{6–8}$** were prepared according to previously published methods.[23,24]

H-L^3: Viscous red oil (14 g, 80%). ^{1}H NMR: δ = 7.73 (s, 1 H, CH=N), 7.70 (s, 1 H, Ar-H), 7.04 (d, J = 7 Hz, 2 H, *m*-2,6-$Me_2C_6H_3$), 6.97 (t, J = 7 Hz, 1 H, *p*-2,6-$Me_2C_6H_3$), 6.91 (d, J = 7 Hz, 1 H, Ar-H), 6.57 (d, J = 7 Hz, 1 H, Ar-H), 5.21 (s, 2 H, OCH_2O), 2.12 (s, 6 H, Me) ppm. ^{13}C{^{1}H} NMR: δ = 161.6, 152.2, 151.9, 149.1, 131.9, 128.6, 127.5, 125.7, 124.1, 108.4, 107.1, 101.7, 18.7 ppm. IR: $\tilde{\nu}$ = 3059 (m), 3013 (m), 2899 (m), 2786 (w), 2041 (w), 1853 (w), 1687 (m), 1636 (s), 1586 (s), 1487 (s), 1447 (s), 1377 (m), 1344 (m), 1251 (s), 1202 (s), 1086 (s), 1038 (s), 932 (s), 851 (m), 809 (s), 767 (s) cm^{-1}. $C_{16}H_{15}NO_2$ (253.30): calcd. C 75.87, H 5.97, N 5.53; found C 75.47, H 5.74, N 5.61.

H-L^5: Viscous yellow oil (19 g, 87%). ^{1}H NMR: δ = 7.90 (s, 1 H, CH=N), 7.80 (s, 1 H, Ar-H), 7.17–7.12 (m, 3 H, 2,6-$Et_2C_6H_3$), 7.02 (d, J = 8 Hz, 1 H, Ar-H), 6.66 (d, J = 8 Hz, 1 H, Ar-H), 5.33 (s, 2 H, OCH_2O), 2.62 (q, J = 8 Hz, 4 H, CH_2CH_3), 1.22 (t, J = 8 Hz, 6 H, CH_2CH_3) ppm. ^{13}C{^{1}H} NMR: δ = 161.4, 151.6, 151.2, 149.3, 133.7, 131.9, 127.0, 125.9, 124.5, 108.6, 107.2, 101.8, 25.6, 15.3 ppm. IR: $\tilde{\nu}$ = 3256 (w), 3224 (w), 3064 (s), 3012 (s), 2967 (s), 2872 (s), 2781 (m), 2698 (w), 2635 (w), 2597 (w), 2551 (w), 2046 (w), 1919 (w), 1858 (w), 1713 (m), 1691 (m), 1643 (s), 1607 (s), 1591 (s), 1552 (m), 1499 (s), 1456 (s), 1385 (s), 1372 (s), 1346 (s), 1263 (s), 1199 (s), 1180 (s), 1123 (s), 1099 (s), 1036 (s), 978 (m), 935 (s), 878 (s), 856 (s), 812 (s), 793 (s), 755 (s), 725 (m), 696 (m) cm^{-1}. $C_{18}H_{19}NO_2$ (281.35): calcd. C 76.84, H 6.81, N 4.98; found C 76.44, H 6.92, N 5.06.

Li-L^3: Tan solid, decomposes readily under similar reaction conditions used to prepare **Li-L$^{1–2,4–8}$** (2.7 g, 67%). ^{1}H NMR: δ = 7.80 (s, 1 H, CH=N), 6.92–6.83 (m, 4 H, Ar-H), 6.53 (d, J = 8 Hz, 1 H, Ar-H), 4.96 (s, 2 H, OCH_2O), 1.93 (s, 6 H, Me) ppm.

Li-L^5: Tan solid (2.9 g, 70%). ^{1}H NMR: δ = 7.91 (s, 1 H, CH=N), 6.96–6.93 (m, 3 H, 2,6-$Et_2C_6H_3$), 6.88 (d, J = 8 Hz, 1 H, Ar-H), 6.61 (d, J = 8 Hz, 1 H, Ar-H), 4.96 (s, 2 H, OCH_2O), 2.33 (q, J = 7 Hz, 4 H, CH_2CH_3), 0.94 (t, J = 7 Hz, 6 H, CH_2CH_3) ppm. ^{13}C{^{1}H} NMR: δ = 175.2, 157.0, 154.9, 150.4, 145.1, 142.9, 135.3, 130.6, 127.0, 125.3, 106.2, 98.8, 25.5, 15.5 ppm. ^{7}Li{^{1}H} NMR: δ = 2.68 ppm. IR: $\tilde{\nu}$ = 1627 (s), 1589 (w), 1552 (s), 1455 (s), 1366 (s), 1322 (m), 1236 (s), 1173 (m), 1113 (w), 1095 (m), 1046 (m), 933 (m), 861 (w), 800 (m), 756 (w) cm^{-1}. $C_{18}H_{18}LiNO_2$ (287.28): calcd. C 75.25, H 6.32, N 4.88; found C 71.94, H 6.12, N 4.81. M.p. 135–136 °C (dec.).

(Li-L^8)$_2$·DME: Tan solid (1.05 g, 67%). ^{1}H NMR: δ = 7.26 (d, J = 8 Hz, 2 H, Ar-H), 7.05–6.99 (m, 6 H, 2,6-*i*$Pr_2C_6H_3$), 6.66 (d, J = 8 Hz, 2 H, Ar-H), 4.81 (s, 4 H, OCH_2O), 3.27 (s, 4 H, MeOCH_2), 3.08 (s, 6 H, OMe), 2.79 (sept, J = 7 Hz, 4 H, CHMe$_2$), 1.92 (s, 6 H, N=CMe), 0.99 (d, J = 7 Hz, 12 H, CHMe_2), 0.90 (d, J = 7 Hz, 12 H, CHMe_2) ppm. ^{13}C{^{1}H} NMR: δ = 177.4, 155.7, 146.6, 144.2, 143.5, 138.4, 125.0, 124.5, 123.6, 104.8, 97.8, 71.8, 58.6, 28.5, 23.7, 23.3, 18.4 ppm (signal of one aromatic carbon atom not observed). ^{7}Li{^{1}H} NMR: δ = 3.84 ppm. IR: $\tilde{\nu}$ = 1604 (s), 1556 (s), 1456 (s), 1375 (s), 1322 (m), 1276 (m), 1243 (s), 1185 (m), 1071 (s), 1038 (s), 931 (m), 819 (w), 776 (m) cm^{-1}. $C_{46}H_{58}Li_2N_2O_6$ (748.84): calcd. C 73.78, H 7.81, N 3.74; found C 73.23, H 7.76, N 3.85. M.p. 73 °C (dec.).

Crystallography: A summary of crystal data and collection parameters for crystal structures of **(Li-L^1)$_4$**, **(Li-L^2)$_4$**, **(Li-L^4·Et$_2$O)$_2$**, **(Li-L^6)$_2$·Et$_2$O**, **(Li-L^6)$_2$**, **(Li-L^7)$_2$**, **(Li-L^8)$_2$**, **(Li-L^8)$_2$·DME**, and **H-L^8** are provided in Tables 5 and 6. Detailed descriptions of data collection and data solution are provided below. ORTEP diagrams were generated with the ORTEP-3 software package.[44] For each sample, a suitable crystal was mounted on a glass fiber by using Paratone-N hydrocarbon oil. The crystal was transferred to a Siemens SMART[45] diffractometer with a CCD area detector, centered in the X-ray beam, and cooled to 140 K by using a nitrogen-flow low-temperature apparatus that had been previously calibrated by a thermocouple placed at the same position as the crystal. An arbitrary hemisphere of data was collected by using 0.3° ω-scans, and the data were integrated by the program SAINT.[46] The final unit-cell parameters were determined by a least-squares refinement of the reflections with $I > 2\sigma(I)$. Data analysis by using Siemens XPREP[47] and the successful solution and refinement of the structure determined the space group. Empirical absorption corrections were applied for **(Li-L^1)$_4$**, **(Li-L^2)$_4$**, **(Li-L^4·Et$_2$O)$_2$**, **(Li-L^6)$_2$·Et$_2$O**, **(Li-L^6)$_2$**, **(Li-L^7)$_2$**, **(Li-L^8)$_2$**, **(Li-L^8)$_2$·DME**, and **H-L^8** by using SADABS.[48] Equivalent reflections were averaged, and the structures were solved by direct methods using the SHELXTL software package.[49] Unless otherwise noted, all non-hydrogen atoms were refined anisotropically.

(Li-L^1)$_4$: X-ray quality crystals were grown from a toluene/pentane (1:1) solution at –20 °C. One quarter of a molecule of toluene was also present in the asymmetric unit. Carbon atoms of the solvent were refined anisotropically and its hydrogen atoms were not modeled. The final cycle of full-matrix least-squares refinement was based on 4814 observed reflections and 685 variable parameters and converged yielding final residuals: R = 0.0545, R_{all} = 0.0893, and GOF = 1.000.

Table 5. Crystallographic data for compounds **(Li-L^1)$_4$**, **(Li-L^2)$_4$**, **(Li-L^4·Et$_2$O)$_2$**, and **(Li-L^6)$_2$·Et$_2$O**.

Compound	**(Li-L^1)$_4$**	**(Li-L^2)$_4$**	**(Li-L^4·Et$_2$O)$_2$**	**(Li-L^6)$_2$·Et$_2$O**
Empirical formula	$C_{56}H_{64}Li_4N_4O_8$·1/4(C_7H_8)	$C_{13}H_{16}LiNO_2$	$C_{21}H_{26}LiNO_3$	$C_{42}H_{50}Li_2N_2O_5$
Formula mass	971.91	225.21	347.37	676.72
Space group	*C*2/*c*	$P\bar{4}2_1c$	$P2_1/n$	$P2_1/n$
Temperature [K]	140	140	140	140
a [Å]	39.324(1)	14.671(2)	11.5286(4)	13.129(3)
b [Å]	13.3815(4)	14.671(2)	13.1880(4)	19.984(4)
c [Å]	21.1315(7)	11.476(2)	12.3759(4)	15.547(3)
α [°]	90	90	90	90
β [°]	91.277(2)	90	94.821(1)	112.816(3)
γ [°]	90	90	90	90
V [Å^3]	11116.9(6)	2470.1(5)	1875.0(1)	3760(1)
Z	8	8	4	4
Density$_{calcd.}$ [g/cm^3]	1.161	1.211	1.231	1.195
Diffractometer	Siemens SMART	Siemens SMART	Siemens SMART	Siemens SMART
Radiation (*λ* [Å])	Mo-K_α (0.71073)	Mo-K_α (0.71073)	Mo-K_α (0.71073)	Mo-K_α (0.71073)
Monochromator	graphite	graphite	graphite	graphite
Detector	CCD area detector	CCD area detector	CCD area detector	CCD area detector
Scan type (width [°])	*ω* (0.3)	*ω* (0.3)	*ω* (0.3)	*ω* (0.3)
Scan speed [s]	60	40	35	30
Reflections measured	hemisphere	hemisphere	hemisphere	hemisphere
2*θ* range [°]	2.08–46.60	3.92–56.04	4.52–56.64	3.46–57.00
Crystal dimensions [mm]	0.26 × 0.19 × 0.09	0.10 × 0.08 × 0.05	0.10 × 0.07 × 0.06	0.10 × 0.07 × 0.06
Reflections measured	44139	26764	20717	37100
Unique reflections	8015	2979	4679	8793
Observations [$I > 2\sigma(I)$]	4814	1529	4074	5559
R_{int}	0.0861	0.1469	0.0386	0.0712
Parameters	685	155	236	479
R	0.0545	0.0612	0.0456	0.0621
R_w	0.1742	0.1744	0.1267	0.1758
R_{all}	0.0893	0.1438	0.0517	0.1078
GoF	1.000	1.001	1.027	1.083

Table 6. Crystallographic data for compounds **(Li-L^6)$_2$**, **(Li-L^7)$_2$**, **(Li-L^8)$_2$**, **(Li-L^8)$_2$·DME**, and **H-L^8**.

Compound	**(Li-L^6)$_2$**	**(Li-L^7)$_2$**	**(Li-L^8)$_2$**	**(Li-L^8)$_2$·DME**	**H-L^8**
Empirical formula	$C_{38}H_{40}Li_2N_2O_4$·C_6H_6	$C_{80}H_{88}Li_4N_4O_8$·C_6H_6	$C_{42}H_{48}Li_2N_2O_4$·1/2(C_7H_8)	$C_{23}H_{29}LiNO_3$	$C_{21}H_{25}NO_2$
Formula mass	680.71	1339.41	704.77	374.41	323.42
Space group	$P2_1/c$	$Pna2_1$	$P\bar{1}$	$P\bar{1}$	$P2_1$
Temperature [K]	140	140	140	140	140
a [Å]	15.106(4)	26.831(1)	11.9324(9)	9.0416(9)	6.983(2)
b [Å]	13.206(3)	23.069(1)	12.7291(9)	9.380(1)	24.325(7)
c [Å]	22.163(6)	12.4740(8)	14.312(1)	12.648(1)	10.799(3)
α [°]	90	90	91.001(2)	75.385(2)	90
β [°]	109.515(5)	90	92.430(2)	86.376(3)	90.296(7)
γ [°]	90	90	112.044(2)	80.736(3)	90
V [Å^3]	4167(2)	7720.9(8)	2011.8(3)	1024.2(2)	1834.3(9)
Z	4	4	2	2	4
Density$_{calcd.}$ [g/cm^3]	1.085	1.152	1.163	1.214	1.171
Diffractometer	Siemens SMART	Siemens SMART	Siemens SMART	Siemens SMART	Siemens SMART
Radiation (*λ* [Å])	Mo-K_α (0.71073)	Mo-K_α (0.71073)	Mo-K_α (0.71073)	Mo-K_α (0.71073)	Mo-K_α (0.71073)
Monochromator	graphite	graphite	graphite	graphite	graphite
Detector	CCD area detector	CCD area detector	CCD area detector	CCD area detector	CCD area detector
Scan type (width [°])	*ω* (0.3)	*ω* (0.3)	*ω* (0.3)	*ω* (0.3)	*ω* (0.3)
Scan speed	30	30	30	30	30
Reflections measured	hemisphere	hemisphere	hemisphere	hemisphere	hemisphere
2*θ* range [°]	3.64–58.46	2.32–56.64	3.46–56.60	4.54–56.64	3.34–57.10
Crystal dimensions [mm]	0.20 × 0.05 × 0.05	0.20 × 0.05 × 0.05	0.10 × 0.10 × 0.05	0.10 × 0.06 × 0.05	0.30 × 0.20 × 0.10
Reflections measured	31766	81349	22547	9904	20833
Unique reflections	10443	19208	9954	4641	8322
Observations [$I > 2\sigma(I)$]	7566	11406	8315	2565	7336
R_{int}	0.0464	0.0624	0.0345	0.0772	0.0238
Parameters	506	967	492	262	433
R	0.0974	0.0562	0.0575	0.0614	0.0408
R_w	0.2803	0.1382	0.1652	0.1839	0.1045
R_{all}	0.1179	0.1125	0.0668	0.1193	0.0476
GoF	1.069	1.004	1.049	0.988	1.033

$(Li\text{-}L^2)_4$: X-ray quality crystals were grown from a saturated diethyl ether solution at –25 °C. The final cycle of full-matrix least-squares refinement was based on 1529 observed reflections and 155 variable parameters and converged yielding final residuals: $R = 0.0612$, $R_{all} = 0.1438$, and GOF = 1.001.

$(Li\text{-}L^4\cdot Et_2O)_2$: X-ray quality crystals were grown from a saturated diethyl ether solution at –25 °C. The final cycle of full-matrix least-squares refinement was based on 4074 observed reflections and 236 variable parameters and converged yielding final residuals: $R = 0.0456$, $R_{all} = 0.0517$, and GOF = 1.027.

$(Li\text{-}L^6)_2\cdot Et_2O$: X-ray quality crystals were grown from a saturated diethyl ether solution at –25 °C. The final cycle of full-matrix least-squares refinement was based on 5559 observed reflections and 479 variable parameters and converged yielding final residuals: $R = 0.0621$, $R_{all} = 0.1078$, and GOF = 1.083.

$(Li\text{-}L^6)_2$: X-ray quality crystals were grown from a saturated benzene solution at room temperature. One molecule of benzene also crystallized in the asymmetric unit. The final cycle of full-matrix least-squares refinement was based on 7566 observed reflections and 506 variable parameters and converged yielding final residuals: $R = 0.0974$, $R_{all} = 0.1179$, and GOF = 1.069.

$(Li\text{-}L^7)_2$: X-ray quality crystals were grown from a saturated benzene solution at room temperature. One benzene molecule cocrystallized; all solvent carbon atoms were modeled anisotropically with hydrogen atoms attached. The final cycle of full-matrix least-squares refinement was based on 11406 observed reflections and 967 variable parameters and converged yielding final residuals: $R = 0.0562$, $R_{all} = 0.1125$, and GOF = 1.004.

$(Li\text{-}L^8)_2$: X-ray quality crystals were grown from a toluene solution layered with pentane. One half of a disordered toluene molecule cocrystallized in the asymmetric unit, and its carbon atoms were modeled anisotropically and hydrogen atoms were not modeled. The final cycle of full-matrix least-squares refinement was based on 8315 observed reflections and 492 variable parameters and converged yielding final residuals: $R = 0.0575$, $R_{all} = 0.0668$, and GOF = 1.049.

$(Li\text{-}L^8)_2\cdot$DME: X-ray quality crystals were grown from a pentane/DME solution at –25 °C. The final cycle of full-matrix least-squares refinement was based on 2565 observed reflections and 262 variable parameters and converged yielding final residuals: $R = 0.0614$, $R_{all} = 0.1193$, and GOF = 0.988.

$H\text{-}L^8$: X-ray quality crystals were grown from a methanol solution. The final cycle of full-matrix least-squares refinement was based on 7336 observed reflections and 433 variable parameters and converged yielding final residuals: $R = 0.0408$, $R_{all} = 0.0476$, and GOF = 1.033.

Supporting Information (see footnote on the first page of this article): ORTEP diagrams for crystal structures of **$(Li\text{-}L^2)_4$**, **$(Li\text{-}L^6)_2$**, **$(Li\text{-}L^6)_2\cdot Et_2O$** polymer, **$(Li\text{-}L^6)_2\cdot Et_2O$** "donor" dimer, **$(Li\text{-}L^7)_2$**, **$(Li\text{-}L^8)_2\cdot$DME** polymer, and **$H\text{-}L^8$**.

Acknowledgments

We gratefully acknowledge The University of Toledo for generous start-up funding, as well as the staff of the Ohio Crystallography Consortium housed at The University of Toledo and Dr. Allen Oliver (University of Notre Dame) for assistance with X-ray crystallography. We also acknowledge Cheryl L. Seambos and Tamam I. Baiz for their early contributions to this chemistry.

[1] H. Gilman, R. L. Bebb, *J. Am. Chem. Soc.* **1939**, *61*, 109–112.
[2] H. Gilman, J. F. Webb, *J. Am. Chem. Soc.* **1940**, *62*, 987–988.
[3] G. Wittig, G. Fuhrmann, *Ber. Dtsch. Chem. Ges.* **1940**, *73*, 1197–1218.
[4] W. Bauer, P. V. Schleyer, *J. Am. Chem. Soc.* **1989**, *111*, 7191–7198.
[5] K. Smith, G. A. El-Hiti, *Curr. Org. Synth.* **2004**, *1*, 253–274.
[6] P. Beak, R. A. Brown, *J. Org. Chem.* **1979**, *44*, 4463–4464.
[7] P. Beak, R. A. Brown, *J. Org. Chem.* **1982**, *47*, 34–46.
[8] D. L. Comins, J. D. Brown, *J. Org. Chem.* **1984**, *49*, 1078–1083.
[9] K. Tomioka, Y. Shioya, Y. Nagaoka, K. Yamada, *J. Org. Chem.* **2001**, *66*, 7051–7054.
[10] L. A. Flippin, J. Berger, J. S. Parnes, M. S. Gudiksen, *J. Org. Chem.* **1996**, *61*, 4812–4815.
[11] L. A. Flippin, J. M. Muchowski, D. S. Carter, *J. Org. Chem.* **1993**, *58*, 2463–2467.
[12] M. A. Forth, M. B. Mitchell, S. A. C. Smith, K. Gombatz, L. Snyder, *J. Org. Chem.* **1994**, *59*, 2616–2619.
[13] D. A. Kovalskiy, V. P. Perevalov, *Chem. Heterocycl. Compd.* **2009**, *45*, 957–964.
[14] M. Stol, D. J. M. Snelders, J. J. M. de Pater, G. P. M. van Klink, H. Kooijman, A. L. Spek, G. van Koten, *Organometallics* **2005**, *24*, 743–749.
[15] P. A. Evans, J. D. Nelson, A. L. Stanley, *J. Org. Chem.* **1995**, *60*, 2298–2301.
[16] S. T. Chadwick, A. Ramirez, L. Gupta, D. B. Collum, *J. Am. Chem. Soc.* **2007**, *129*, 2259–2268.
[17] K. L. Jantzi, I. A. Guzei, H. J. Reich, *Organometallics* **2006**, *25*, 5390–5395.
[18] F. E. Ziegler, K. W. Fowler, *J. Org. Chem.* **1976**, *41*, 1564–1566.
[19] F. E. Ziegler, I. Chliwner, K. W. Fowler, S. J. Kanfer, S. J. Kuo, N. D. Sinha, *J. Am. Chem. Soc.* **1980**, *102*, 790–798.
[20] M. Khaldi, F. Chretien, Y. Chapleur, *Bull. Soc. Chim. Fr.* **1996**, *133*, 7–13.
[21] M. Pfeffer, E. P. Urriolabeitia, A. Decian, J. Fischer, *J. Organomet. Chem.* **1995**, *494*, 187–193.
[22] B. M. Trost, M. Reiffen, M. Crimmin, *J. Am. Chem. Soc.* **1979**, *101*, 257–259.
[23] A. Neshat, C. L. Seambos, J. F. Beck, J. A. R. Schmidt, *Dalton Trans.* **2009**, 4987–5000.
[24] T. I. Baiz, J. A. R. Schmidt, *Organometallics* **2007**, *26*, 4094–4097.
[25] J. F. Beck, T. I. Baiz, A. Neshat, J. A. R. Schmidt, *Dalton Trans.* **2009**, 5001–5008.
[26] J. B. Lambert, E. P. Mazzola, *Nuclear Magnetic Resonance Spectroscopy*, Pearson Education Inc., Upper Saddle River, NJ, **2004**.
[27] D. L. Pavia, G. M. Lampman, G. S. Kriz, *Introduction to Spectroscopy*, 3rd ed., Thomson Learning, Inc., Belmont, CA, **2001**.
[28] N. H. Martin, R. M. Floyd, H. L. Woodcock, S. Huffman, C. K. Lee, *J. Mol. Graphics Modell.* **2008**, *26*, 1125–1130.
[29] M. Skowronskaptasinska, W. Verboom, D. N. Reinhoudt, *J. Org. Chem.* **1985**, *50*, 2690–2698.
[30] M. A. Nichols, P. G. Williard, *J. Am. Chem. Soc.* **1993**, *115*, 1568–1572.
[31] D. B. Collum, *Acc. Chem. Res.* **1992**, *25*, 448–454.
[32] A. W. Addison, T. N. Rao, J. Reedijk, J. Vanrijn, G. C. Verschoor, *J. Chem. Soc., Dalton Trans.* **1984**, 1349–1356.
[33] J. Betz, F. Hampel, W. Bauer, *J. Chem. Soc., Dalton Trans.* **2001**, 1876–1879.
[34] I. Fernandez, P. Ona-Burgos, J. M. Oliva, F. Lopez-Ortiz, *J. Am. Chem. Soc.* **2010**, *132*, 5193–5204.
[35] C. Gaul, P. I. Arvidsson, W. Bauer, R. E. Gawley, D. Seebach, *Chem. Eur. J.* **2001**, *7*, 4117–4125.
[36] J. Betz, W. Bauer, *J. Am. Chem. Soc.* **2002**, *124*, 8699–8706.
[37] R. E. Dinnebier, U. Behrens, F. Olbrich, *J. Am. Chem. Soc.* **1998**, *120*, 1430–1433.
[38] J. Jastrzebski, G. Van Koten, K. Goubitz, C. Arlen, M. Pfeffer, *J. Organomet. Chem.* **1983**, *246*, C75–C79.

[39] S. Harder, P. F. Ekhart, L. Brandsma, J. A. Kanters, A. J. M. Duisenberg, P. v. R. Schleyer, *Organometallics* **1992**, *11*, 2623–2627.
[40] M. Linnert, C. Bruhn, T. Ruffer, H. Schmidt, D. Steinborn, *Organometallics* **2004**, *23*, 3668–3673.
[41] A. Domenicano, A. Vaciago, C. A. Coulson, *Acta Crystallogr., Sect. B: Struct. Sci.* **1975**, *31*, 1630–1641.
[42] J. Betz, F. Hampel, W. Bauer, *Org. Lett.* **2000**, *2*, 3805–3807.
[43] H. A. Bent, *Chem. Rev.* **1961**, *61*, 275–311.
[44] C. L. Barnes, *J. Appl. Crystallogr.* **1997**, *30*, 568–568.
[45] *SMART: Area-Detector Software Package*, v. 5.625, Bruker AXS, Inc., Madison, WI, **1997**–**2001**.
[46] *SAINT: SAX Area-Detector Integration Program*, v. 6.22, Bruker AXS, Inc., Madison, WI, **1997**–**2001**.
[47] *XPREP: Reciprocal Space Exploration Program*, v. 6.12, Bruker AXS, Inc., Madison, WI, **2001**.
[48] *SADABS, Bruker/Siemens Area Detector Absorption Program*, v. 2.03, Bruker AXS, Inc., Madison, WI, **2001**.
[49] *SHELXTL-97, Structure Solution Program*, v. 6.10, Bruker AXS, Inc., Madison, WI, **2000**.

Received: May 10, 2010
Published Online: September 27, 2010

